









Isotopic cross sections in fragmentation reactions of $^{12,14}\text{C}$, $^{14,16}\text{N}$, and ^{16}O projectiles on a carbon target

Bo Mei ^{1,2,*}, Yutian Guan,¹ Ningxin Zeng,¹ Ziyi Mai,¹ Jiajun Tu ¹, Tianjun Yu,¹ Shitao Wang ^{2,†}, Xueheng Zhang,² Peng Ma,² Xiaodong Xu ², Xiaolin Tu,² Yazhou Sun ², Zhiyu Sun ², Shuwen Tang,² Yuhong Yu,² Fang Fang,² Duo Yan,² Shuya Jin ², Yixuan Zhao ², Shaobo Ma,² and Yongjie Zhang²

¹*Sino-French Institute of Nuclear Engineering and Technology, Sun Yat-sen University, Zhuhai 519082, China*

²*Institute of Modern Physics, Chinese Academy of Sciences, Lanzhou 730000, China*



(Received 5 May 2023; accepted 18 August 2023; published 1 September 2023)

Systematic measurements of 51 isotopic cross sections from fragmentation reactions of 240 MeV/nucleon $^{12,14}\text{C}$, $^{14,16}\text{N}$, and ^{16}O projectiles on a carbon target were performed at the RIBLL2 separator and the external target facility (ETF) of the Heavy-Ion Research Facility in Lanzhou (HIRFL). Our experimental cross sections produced by fragmentation of three stable projectiles, i.e., ^{12}C , ^{14}N , and ^{16}O , were compared with some previous experimental data measured at different energies. The comparison indicates that our experimental data are in generally good agreement with previous experimental data. Tens of new isotopic cross sections produced by fragmentation of two unstable projectiles ^{14}C and ^{16}N were also measured in this work. All cross sections measured in this work were used for benchmarking three fragmentation models, i.e., ABRABLA, NUCFRG, and FRACS. Most experimental data can be well reproduced by these fragmentation models, but there are severe discrepancies for some isotopic cross sections from fragmentation of unstable projectiles.

DOI: [10.1103/PhysRevC.108.034602](https://doi.org/10.1103/PhysRevC.108.034602)

I. INTRODUCTION

Fragmentation reactions above tens of MeV/nucleon have been widely applied in many nuclear physics experiments aimed at producing and investigating exotic nuclei away from stability. Extensive isotopic cross sections (yields) from fragmentation reactions with different projectile-target combinations have been measured at the A1900 separator at MSU [1–4], the FRS separator at GSI [5–9], the BigRIPS separator at RIKEN [10–14], and the HIRFL-CSR facility at IMP [15–19]. To harvest (new) unstable isotopes near the drip lines, the fragmentation reaction will also be employed as one of the most powerful methods in future experiments at next generation radioactive beam facilities, e.g., FRIB at MSU [20], FAIR at GSI [21], and HIAF at IMP [22]. Isotopic cross sections in fragmentation reactions are critical input parameters for estimating production yields of exotic nuclei of interest and designing nuclear physics experiments in the above facilities. Furthermore, fragmentation reactions play an important part in some applications, such as cancer therapy with heavy ions, production of medical radioisotopes, cosmic-ray propagation, and radiation protection in space. Accurate fragmentation cross sections are essential nuclear data required in these applications.

Some light ions (e.g., ^{12}C and ^{16}O) have been explored for cancer therapy, where reliable fragmentation cross sections are critical for the dose optimization and treatment

planning. However, few isotopic cross sections have been measured in fragmentation reactions of these light projectiles (see, e.g., Refs. [23–27]) and significant discrepancies are observed for cross sections measured in different experiments. For instance, a significant difference (a factor of about 10) has been observed between the experimental cross section of ^7Be produced by ^{14}N fragmentation in Ref. [27] and that measured in Ref. [24]. In the case of ^{12}C fragmentation reactions, cross sections of ^{11}B measured in Ref. [25] are about 50% smaller than those from other experiments [23,24,26,27]). Considering these deficiencies and discrepancies in previous experimental data, new measurements of isotopic cross sections should be performed for fragmentation of light projectiles.

With the development of modern radioactive ion beam facilities, reactions of light unstable ions at medium energies have been carried out recently [27,28]. Although nucleon-removal cross sections in reactions induced by light exotic nuclei have been extensively investigated by using such facilities, systematic measurements of production cross sections of other residual fragments are still very scarce. More experimental studies of fragmentation reactions with light unstable projectiles are very welcome for understanding the structure of these unstable nuclei and their reaction mechanism.

Theoretically, various fragmentation models have been developed to calculate isotopic cross sections. First, some empirical models, such as the parametrization FRACS [29] considering the odd-even staggering (OES) observed in extensive experimental data [16,17,19,29–31] and the parametrization EPAX without the OES [32], have been developed for fast and accurate calculations of isotopic cross sections. Furthermore,

*meibo5@mail.sysu.edu.cn

†wangshitao@impcas.ac.cn

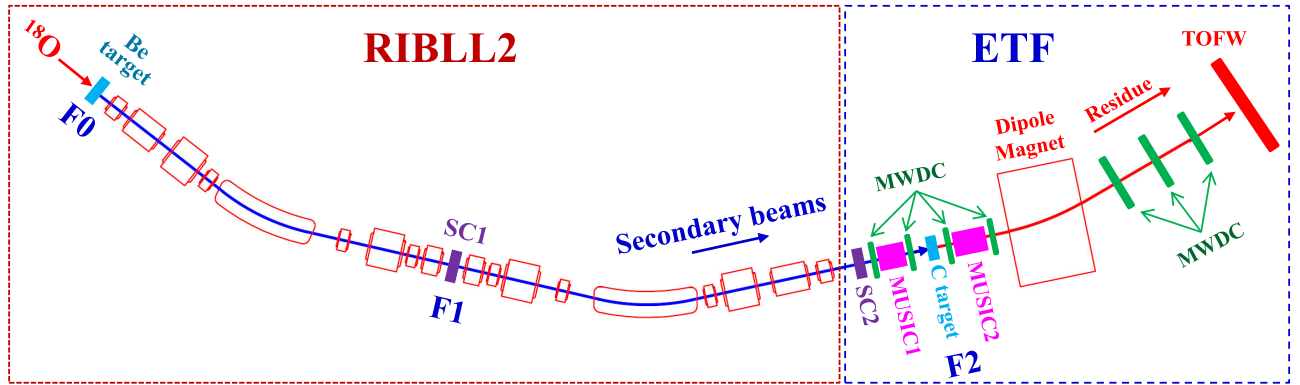


FIG. 1. Schematic view of the experimental facility including RIBLL2 and ETF used in this experiment.

some fragmentation models based on the abrasion-ablation process, such as ABRABLA [33], NUCFRG2 [34], and the LISE++ abrasion-ablation model [35], have been widely applied for fragmentation reactions. Finally, considering the universality of the OES in extensive experimental isotopic cross sections along a constant isospin chain [16,17,30,31], some OES relations have been proposed and applied for interpolating or extrapolating of isotopic cross sections [36,37]. However, the prediction power of these fragmentation models is still unclear for fragmentation of light projectiles, especially for unstable ones, due to the lack of experimental data. Considering that the OES effect caused by nuclear pairing and shell structures is particularly strong for light nuclei [30,31], more experimental cross sections of light nuclei produced by fragmentation of light projectiles are very suitable for benchmarking fragmentation models.

In this work, we report systematic measurements of many isotopic cross sections from several fragmentation reactions of 240 MeV/nucleon $^{12,14}\text{C}$, $^{14,16}\text{N}$, and ^{16}O projectiles on a carbon target, which were performed at RIBLL2 separator and the External Target Facility (ETF) at IMP. These isotopic cross sections determined in our experiment are compared with some existing experimental data from fragmentation of ^{12}C , ^{14}N , and ^{16}O projectiles at different energies. To validate fragmentation models, our experimental data are also compared with isotopic cross sections predicted by three fragmentation models, i.e., FRACS, NUCFRG2, and ABRABLA.

II. EXPERIMENT AND DATA ANALYSIS

This experiment was performed at the RIBLL2 separator and the External Target Facility (ETF) [38,39] at the Heavy-Ion Research Facility in Lanzhou (HIRFL), where several nucleon-knockout reactions of light nuclei were measured successfully [40–42]. The primary ^{18}O beam was accelerated to 280 MeV/nucleon by the main Cooler Storage Ring (CSRm) of HIRFL. Then, the ^{18}O beam was transported to RIBLL2 and directed onto a Be target with a thickness of 15 mm, which was positioned at the entrance of RIBLL2, as displayed in Fig. 1. Secondary radioactive beams produced by ^{18}O fragmentation were separated at RIBLL2 according to their magnetic rigidities. The magnetic rigidity $B\rho$ of RIBLL2 was optimized for ^{12}C and ^{14}C in two different settings.

Next, the separated cocktail beams were delivered to ETF and focused onto a C target with a thickness of 900 mg/cm². The secondary beams were identified by using the TOF- ΔE method. The time-of-flight $\text{TOF}_{\text{SC1} \rightarrow \text{SC2}}$ was determined by a pair of plastic scintillator detectors (SC1 and SC2). The particle energy loss (ΔE) was obtained by a multiple sampling ionization chamber (MUSIC1) placed at the entrance of the ETF. Figure 2 presents an example of the particle identification (PID) spectrum for the cocktail beams optimized for ^{14}C , where different isotopes (e.g., ^{16}N , ^{14}C , ^{12}B , ^{11}B , and ^9Be) are distinctly separated.

Downstream of the 900 mg/cm² C target at ETF, the $B\rho$ -TOF- ΔE method was applied to identify the ions (reaction products and unreacted beam) on an event-by-event basis. The energy loss ΔE of ions was determined from the multiple sampling ionization chamber (MUSIC2) downstream of the 900 mg/cm² C target. The $\text{TOF}_{\text{SC2} \rightarrow \text{TOFW}}$ of ions was measured between a plastic scintillator (SC2) and a plastic scintillator wall (TOFW) with an active area of 120×120 cm². The $B\rho$ of ions was reconstructed from particle positions measured by two multiwire drift chambers (MWDCs)

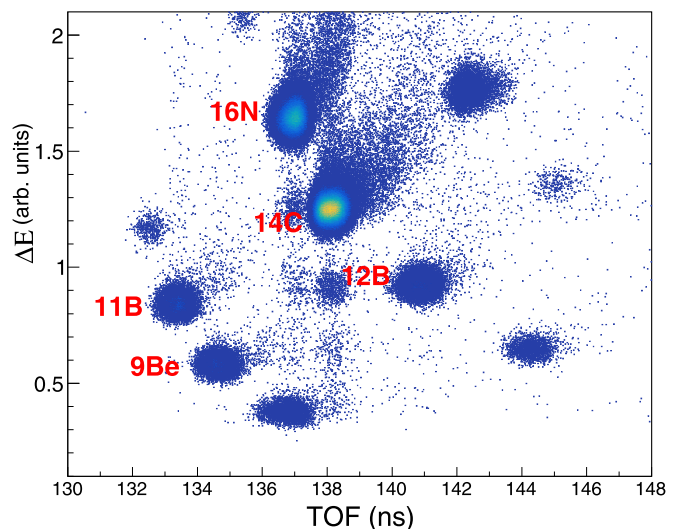


FIG. 2. Particle identification spectrum for secondary beams, e.g., ^{14}C and ^{16}N .

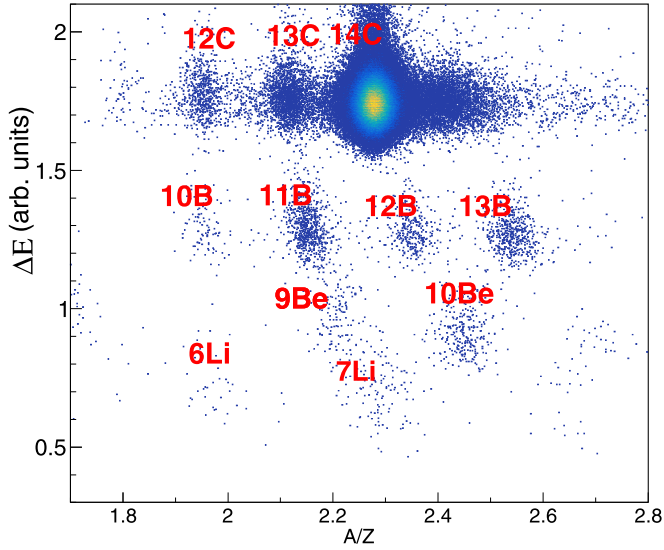


FIG. 3. Particle identification spectrum for isotopes produced by ^{14}C fragmentation on a C target.

placed upstream and three MWDCs placed downstream of the dipole magnet [39]. Isotopes produced by fragmentation of the secondary beam can be identified unambiguously. As a typical example, Fig. 3 presents a clear identification for various isotopes produced by ^{14}C fragmentation on the C target.

To subtract background contributions from other materials of the beamline detectors, empty target measurements without the C target were also performed under the same beam settings as the above runs employing the C target. Final production cross sections of isotopes produced by the C target are determined by subtracting contributions of background events measured in the empty target runs.

III. RESULTS AND DISCUSSION

The production cross section of one isotope can be determined according to

$$\sigma_i = \frac{N_i}{N_p t \epsilon}, \quad (1)$$

where N_p and N_i stand for the event numbers of the projectile and the produced isotope, respectively. ϵ is the total efficiency accounting for the detection efficiency, geometric efficiency, and event loss due to the target-thickness effect. The detection efficiency is evaluated from measurements of different secondary beams without the C target [40,42,43]. Additionally, the geometric efficiency is determined by carefully studying the position distribution of each isotope in TOFW, similar to the method used in Ref. [43]. This geometric efficiency is nearly 100% for most fragments, except for few isotopes out the acceptance of detectors. Finally, small corrections for the target-thickness effect are also considered, following our previous works [40,42].

More than 50 isotopic cross sections from fragmentation of $^{12,14}\text{C}$, $^{14,16}\text{N}$, and ^{16}O projectiles determined by Eq. (1) are listed in Table I, where the background contributions from the

TABLE I. Production cross sections of some isotopes produced by fragmentation of $^{12,14}\text{C}$, $^{14,16}\text{N}$, and ^{16}O projectiles on a carbon target. Errors of measured cross sections are also indicated.

Projectile	Fragment	Cross section (mb)
^{12}C	^{11}C	60.64 ± 13.1
^{12}C	^{10}C	4.86 ± 4.27
^{12}C	^{11}B	63.91 ± 6.55
^{12}C	^{10}B	37.88 ± 5.2
^{12}C	^{10}Be	6.77 ± 1.59
^{12}C	^9Be	9.48 ± 1.89
^{12}C	^7Be	23.18 ± 3.72
^{12}C	^6Li	30.58 ± 9.01
^{14}N	^{13}C	22.93 ± 4.27
^{14}N	^{12}C	129.03 ± 14.02
^{14}N	^{11}C	22.02 ± 4.34
^{14}N	^{11}B	38.15 ± 5.33
^{14}N	^{10}B	23.18 ± 4.37
^{14}N	^9Be	8.09 ± 2.56
^{14}N	^7Be	20.79 ± 3.41
^{14}N	^7Li	24.89 ± 14.0
^{14}N	^6Li	29.35 ± 14.4
^{16}O	^{15}N	61.6 ± 4.97
^{16}O	^{14}N	48.06 ± 4.47
^{16}O	^{13}N	7.77 ± 1.29
^{16}O	^{14}C	8.02 ± 1.05
^{16}O	^{13}C	32.1 ± 2.9
^{16}O	^{12}C	61.73 ± 4.82
^{16}O	^{11}C	16.99 ± 2.1
^{16}O	^{11}B	33.51 ± 3.01
^{16}O	^{10}B	21.89 ± 1.94
^{16}O	^9Be	9.29 ± 1.43
^{16}O	^7Be	20.06 ± 2.14
^{16}O	^6Li	29.6 ± 5.5
^{14}C	^{13}C	73.62 ± 12.55
^{14}C	^{12}C	26.43 ± 5.97
^{14}C	^{12}B	22.68 ± 2.18
^{14}C	^{11}B	55.74 ± 4.13
^{14}C	^{10}B	13.75 ± 1.64
^{14}C	^{10}Be	24.46 ± 2.24
^{14}C	^9Be	11.67 ± 1.41
^{14}C	^7Li	43.91 ± 5.25
^{14}C	^6Li	23.28 ± 4.58
^{16}N	^{15}N	72.57 ± 14.25
^{16}N	^{14}N	21.24 ± 8.08
^{16}N	^{14}C	54.24 ± 4.94
^{16}N	^{13}C	56.52 ± 5.06
^{16}N	^{12}C	34.88 ± 3.79
^{16}N	^{13}B	7.79 ± 1.62
^{16}N	^{12}B	15.42 ± 2.2
^{16}N	^{11}B	51.13 ± 4.71
^{16}N	^{10}B	12.96 ± 2.11
^{16}N	^{10}Be	14.98 ± 2.17
^{16}N	^9Be	21.9 ± 2.54
^{16}N	^7Li	37.33 ± 6.31
^{16}N	^6Li	26.25 ± 5.81

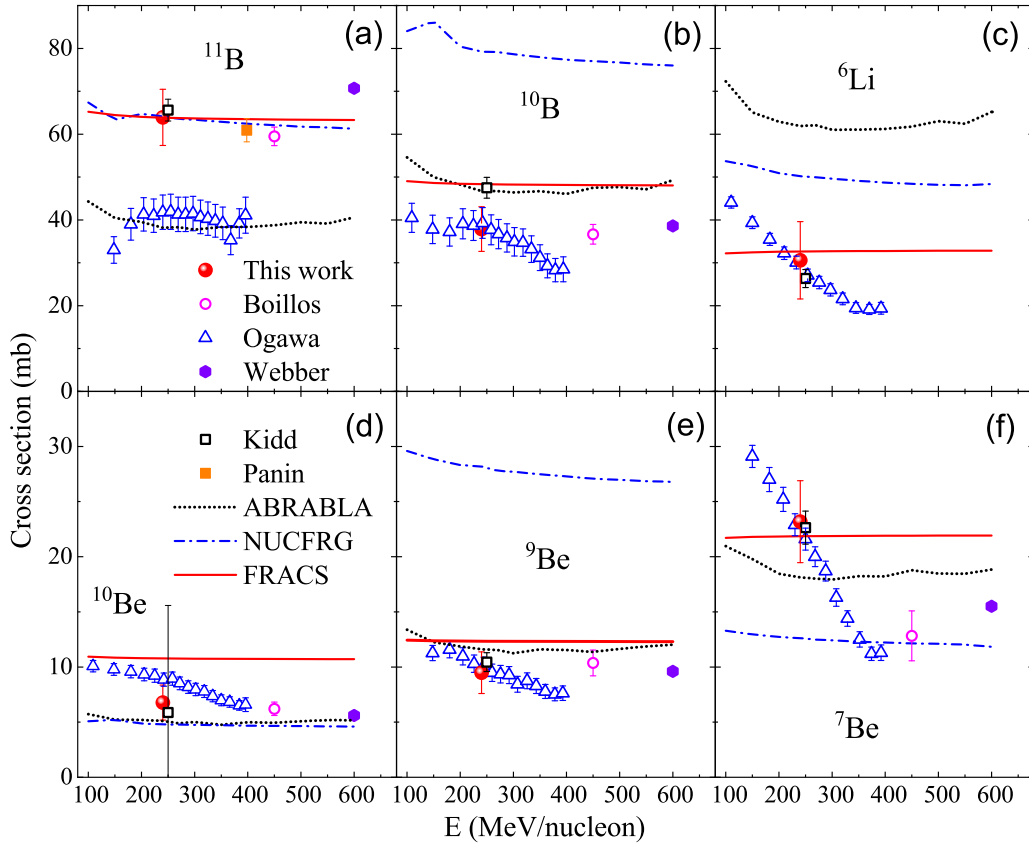


FIG. 4. Energy dependence of isotopic cross sections of $^{11,10}\text{B}$, $^{10,9,7}\text{Be}$, and ^6Li produced by ^{12}C fragmentation on a carbon target. Cross sections measured in this work are compared with those measured in other experiments [23–27] as well as calculations by different models, i.e., ABRABLA, NUCFRG, and FRACS. The relative errors for cross sections measured by Webber *et al.* [24] are estimated to be around 10%, and are not shown.

empty target were subtracted by using the empty target runs. For most of our experimental cross sections, their uncertainties are below 20%, which contain statistical and systematic contributions. In the following, our experimental cross sections from fragmentation of ^{12}C , ^{14}N , and ^{16}O projectiles will be compared with some previous experimental data measured at different energies. In this work, tens of isotopic cross sections produced by fragmentation of two unstable projectiles ^{14}C and ^{16}N are measured for the first time. All these experimental data will be used to validate several fragmentation models.

A. Fragmentation of ^{12}C

The energy dependence of production cross sections of some light isotopes produced by fragmentation of ^{12}C projectiles on a carbon target has been studied over a wide energy range in previous experiments [25,27]. However, some discrepancies have been observed in these experimental results [25,27]. To check the energy dependence, experimental cross sections of several isotopes ($^{11,10}\text{B}$, $^{10,9,7}\text{Be}$, and ^6Li) determined in this work are compared with those measured in previous experiments over a broad energy range [23–27], as shown in Fig. 4.

According to Fig. 4, cross sections of ^{11}B , $^{10,9,7}\text{Be}$, and ^6Li obtained in our experiment at 240 MeV/nucleon are in

excellent agreement with those measured by Kidd *et al.* at 250 MeV/nucleon [23]. For ^{10}B , our cross section agrees with those measured by Ogawa *et al.* over a broad energy range (between 100 and 400 MeV/nucleon) [25] and other experimental data at higher energies, i.e., 450 MeV/nucleon obtained by Boillos *et al.* [27] and 600 MeV/nucleon reported by Webber *et al.* [24], while the cross section measured in Ref. [23] is slightly larger than other experimental data. For ^{11}B , our experimental cross section is in good agreement with other experimental data at various energies, i.e., 250 MeV/nucleon from Kidd *et al.* [23], 400 MeV/nucleon from Panin *et al.* [26], 450 MeV/nucleon from Boillos *et al.* [27], and 600 MeV/nucleon from Webber *et al.* [24], except for those reported by Ogawa *et al.* [25], which are systematically smaller. All experimental data in Fig. 4 indicate that cross sections of $^{11,10}\text{B}$ and $^{10,9}\text{Be}$ above 200 MeV/nucleon do not show evident energy dependence, while the cross section of ^7Be seems to display an obvious energy dependence. For ^6Li , more experimental cross sections at different energies are required to check the energy dependence.

It should be mentioned that the production cross sections of $^{11,10}\text{C}$ were also measured in this work, as listed in Table I. Our experimental cross sections are in good agreement with those [55.97(4.06) and 5.33(0.81) mb] reported by Kidd *et al.*

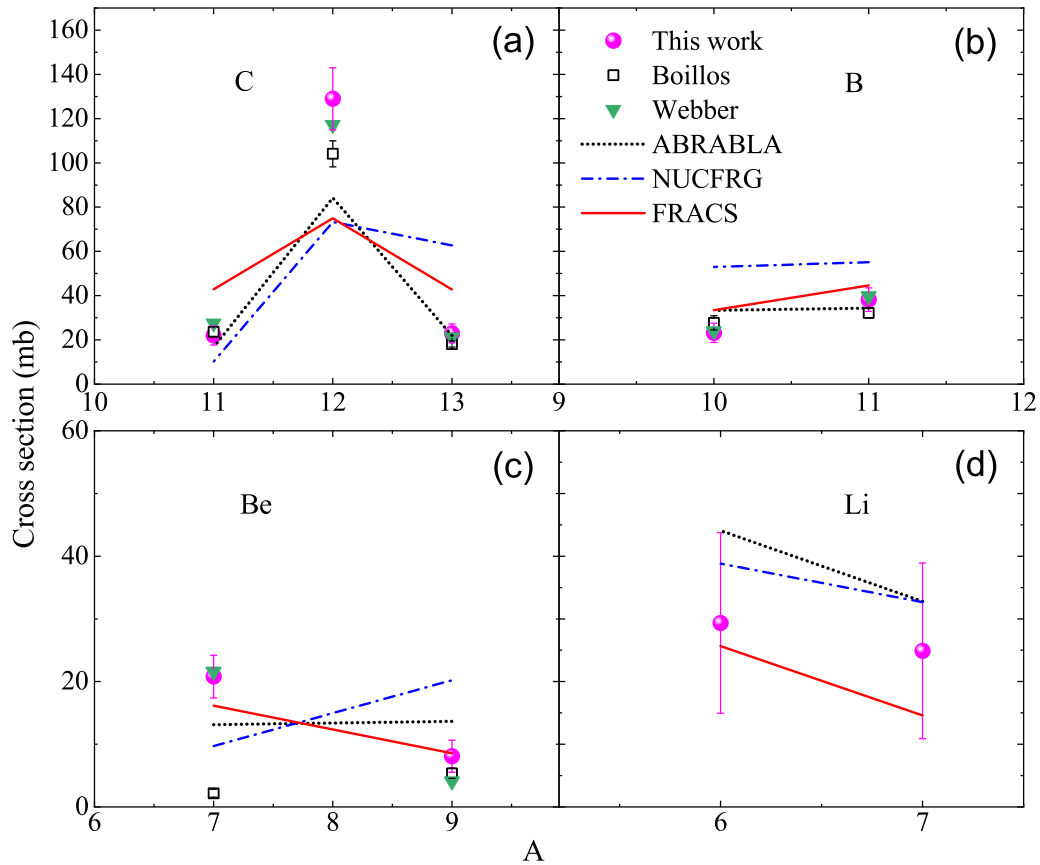


FIG. 5. Production cross sections of C, B, Be, and Li isotopes produced by ^{14}N fragmentation on a carbon target. Cross sections measured in this work are compared with those measured in other experiments [24,27] as well as calculations by different models, i.e., ABRABLA, NUCFRG, and FRACS.

at 250 MeV/nucleon [23], although they are not shown in Fig. 4.

The above experimental data are also compared with predictions by three fragmentation models, i.e., ABRABLA [33], NUCFRG [34], and FRACS [29]. In general, cross sections calculated by these fragmentation models agree with most experimental data within a factor of 2. However, these models still have difficulties in reproducing some experimental data, and a few large discrepancies are observed. For instance, cross sections of ^{10}B , ^9Be , and ^6Li calculated by NUCFRG [34] are systematically larger than all experimental results. As illustrated in Fig. 4, cross sections above 200 MeV/nucleon calculated by ABRABLA [33], NUCFRG [34], and FRACS [29] are almost independent of the projectile energy.

B. Fragmentation of ^{14}N

Production cross sections of C, B, Be, and Li isotopes produced by 240 MeV/nucleon ^{14}N fragmentation on a carbon target were measured in this work. Our experimental data are also compared with cross sections measured at slightly higher energies, i.e., those around 450 MeV/nucleon [27] and near 600 MeV/nucleon [24]. For C, B, and Be isotopes displayed in Fig. 5, our experimental cross sections measured

at 240 MeV/nucleon show very good agreement with most experimental data at higher energies within their uncertainties. For ^7Be , our experimental cross section agrees remarkable with that reported by Webber *et al.* in Ref. [24], while the cross section measured by Boillos *et al.* in Ref. [27] is significantly lower by a factor of 10. This severely deviation could be attributed to the underestimation of the ^7Be cross section in Ref. [27] (see detailed explanations in Ref. [27]). A comparison of all cross sections from different energies indicates that these isotopic cross sections seem to be independent of energy in this energy region. All experimental data are also compared with cross sections calculated by ABRABLA [33], NUCFRG [34], and FRACS [29]. These model calculations agree with most experimental data within a factor of 2, including cross sections of $^{7,6}\text{Li}$ first measured in this work. However, some discrepancies are also observed for some isotopic cross sections. For example, experimental cross sections of $^{9,7}\text{Be}$ cannot be well reproduced by ABRABLA [33] and NUCFRG [34].

C. Fragmentation of ^{16}O

Production cross sections of N, C, B, Be, and Li isotopes produced by 240 MeV/nucleon ^{16}O fragmentation on a carbon target were measured in this work. Our experimental

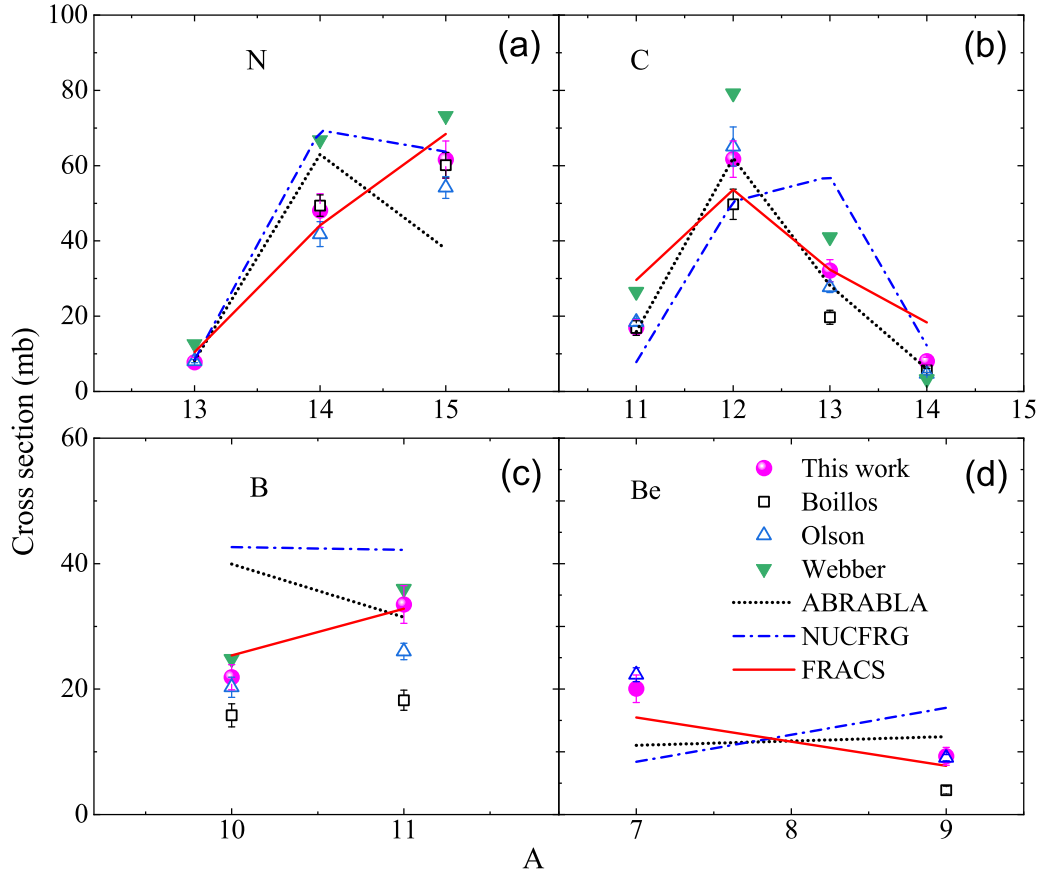


FIG. 6. Production cross sections of N, C, B, and Be isotopes produced by ^{16}O fragmentation on a carbon target. Cross sections measured in this work are compared with those measured in other experiments [24,27,44] as well as calculations by different models, i.e., ABRABLA, NUCFRG, and FRACS.

cross sections are compared with previous experimental data measured at different energies. According to comparisons shown in Fig. 6, our experimental data generally agree with most cross sections measured at higher energies, i.e., those near 450 MeV/nucleon [27], about 600 MeV/nucleon [24], and around 2.1 GeV/nucleon [44]. Our experimental cross sections of $^{13,14,15}\text{N}$ are in excellent agreement with those reported in Refs. [27,44], while cross sections of $^{14,15}\text{N}$ measured by Webber *et al.* in Ref. [24] are much higher. For C, B, and Be isotopes, our experimental data agree very well with cross sections measured by Olson *et al.* at 2.1 GeV/nucleon [44]. For some isotopes, e.g., ^{13}C , $^{10,11}\text{B}$, and ^9Be , cross sections measured by Boillos *et al.* in Ref. [27] seem to be lower than those from other experiments. For $^{14,15}\text{N}$ and $^{11,12,13}\text{C}$, experimental cross sections reported in Ref. [24] are much higher than those from other experiments. The cross section of ^6Li measured in this work is listed in Table I but not given in Fig. 6, and it is consistent with that (35.9 ± 2.9 mb) measured by Olson *et al.* at 2.1 GeV/nucleon [44].

Furthermore, these experimental data are compared with predictions by some fragmentation models. Isotopic cross sections calculated by ABRABLA [33], NUCFRG [34], and FRACS [29] are in good agreement with most experimental data within a factor of 2. However, model predictions

present evident discrepancies for some isotopes (see, e.g., ABRABLA [33] predictions for ^{10}B as well as ^{15}N , and NUCFRG [34] predictions for $^{7,9}\text{Be}$, $^{10,11}\text{B}$, and ^{13}C), according to comparisons with experimental data.

D. Fragmentation of ^{14}C

Cross sections of some isotopes, i.e., $^{13,12}\text{C}$, $^{12,11,10}\text{B}$, $^{10,9}\text{Be}$, and $^{7,6}\text{Li}$, produced by 240 MeV/nucleon ^{14}C fragmentation on a carbon target were measured in our experiment. In Fig. 7, our experimental data are also compared with predictions by three fragmentation models, i.e., ABRABLA, NUCFRG, and FRACS. Isotopic cross sections calculated by FRACS [29] agree with most experimental data, except for the production cross sections of ^{13}C and ^7Li . ^{13}C is produced by the single-neutron removal reaction, which is not well described by FRACS. ABRABLA [33] cannot reproduce the variation tendency of experimental cross sections of C and Be isotopes with the increase of mass number. Similarly, NUCFRG can not describe the variation tendency of measured cross sections of the C, B, Be, and Li isotopes. The above comparisons indicate that these fragmentation models should be improved to reproduce isotopic cross sections produced by fragmentation of the unstable projectile ^{14}C .

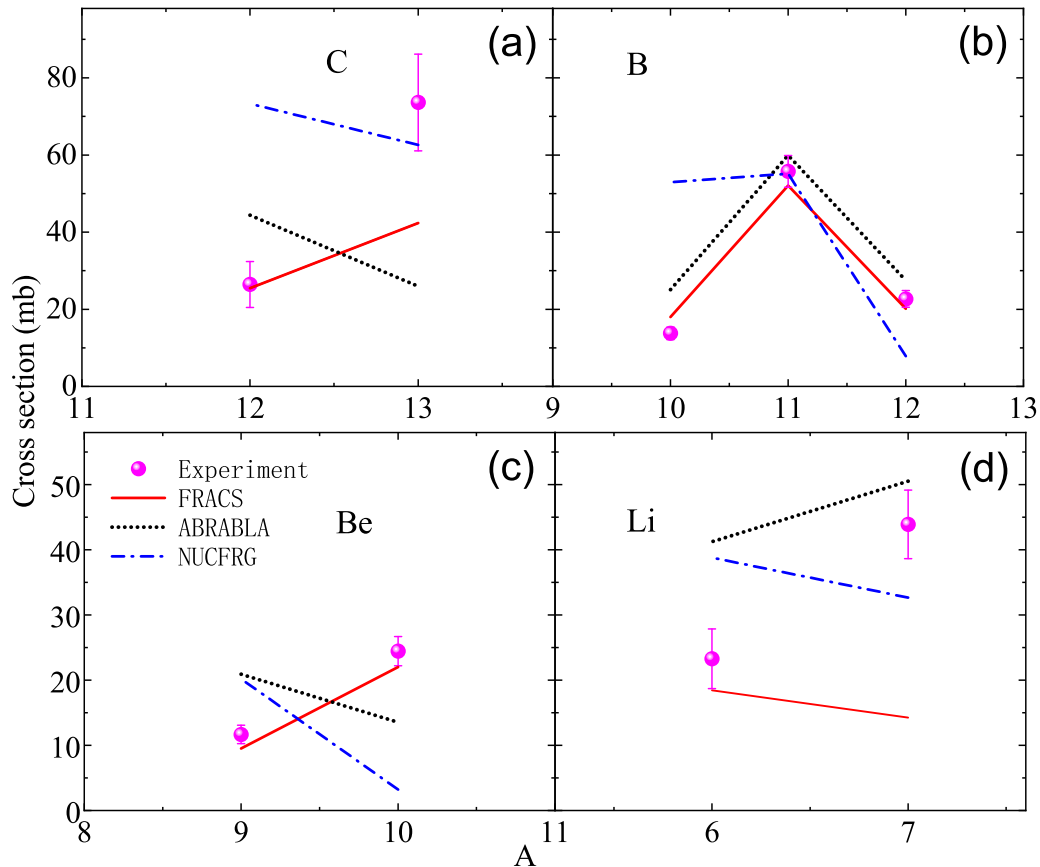


FIG. 7. Production cross sections of C, B, Be, and Li isotopes produced by ^{14}C fragmentation on a carbon target. Cross sections measured in this work are compared with calculations by different models, i.e., ABRABLA, NUCFRG, and FRACS.

E. Fragmentation of ^{16}N

Production cross sections of some isotopes, i.e., $^{15,14}\text{N}$, $^{14,13,12}\text{C}$, $^{13,12,11,10}\text{B}$, $^{10,9}\text{Be}$, and $^{7,6}\text{Li}$, produced by 240 MeV/nucleon ^{16}N fragmentation on a carbon target were measured in our experiment. In Fig. 8, our experimental data are compared with predictions by three fragmentation models, i.e., ABRABLA, NUCFRG, and FRACS, since there are no other experimental data. In general, FRACS predictions can reproduce most experimental data within a factor of 2, although cross sections of ^{13}C , ^9Be , and ^7Li are not well reproduced. Compared with measured cross sections, predictions of NUCFRG show large discrepancies, e.g., for ^{14}N , ^{13}B , and ^{10}Be . ABRABLA can reproduce experimental cross sections of some B, Be, and Li isotopes, while some discrepancies are observed for cross sections of some N and C isotopes.

All comparisons given in Figs. 4–6 indicate that our experimental cross sections from fragmentation of ^{12}C , ^{14}N , and ^{16}O projectiles are in excellent agreement with most existing data measured at different energies. Furthermore, our experimental cross sections confirm and clarify some discrepancies in previous experimental data; see, e.g., cross sections of ^7Be measured in two previous ^{14}N fragmentation experiments. Our experimental results from $^{12,14}\text{C}$, $^{14,16}\text{N}$, and ^{16}O fragmentation reactions are

also applied to validate three fragmentation models, i.e., ABRABLA, NUCFRG, and FRACS. These model calculations are in generally good agreement with most of our experimental data within a factor of 2, although large discrepancies are also observed for some isotopic cross sections.

IV. SUMMARY

In summary, secondary beams produced by ^{18}O fragmentation on a Be target were used to study fragmentation reactions at the RIBLL2-ETF of HIRFL. More than 50 isotopic cross sections of residual nuclei produced by fragmentation of different secondary beams, i.e., $^{12,14}\text{C}$, $^{14,16}\text{N}$, and ^{16}O , on a carbon target were measured under two different settings optimized for ^{12}C and ^{14}C beams, respectively. For fragmentation of stable projectiles ^{12}C , ^{14}N , and ^{16}O , our experimental cross sections were compared with some previous experimental data measured at different energies. Our experimental data are in very good agreement with most existing experimental data within their uncertainties and clarify some discrepancies in previous experimental data; see, e.g., the production cross section of ^7Be measured in two previous ^{14}N fragmentation experiments shown in Fig. 5. Furthermore, dozens of isotopic cross sections produced by fragmentation of unstable projectiles ^{14}C and ^{16}N were first measured in this work.

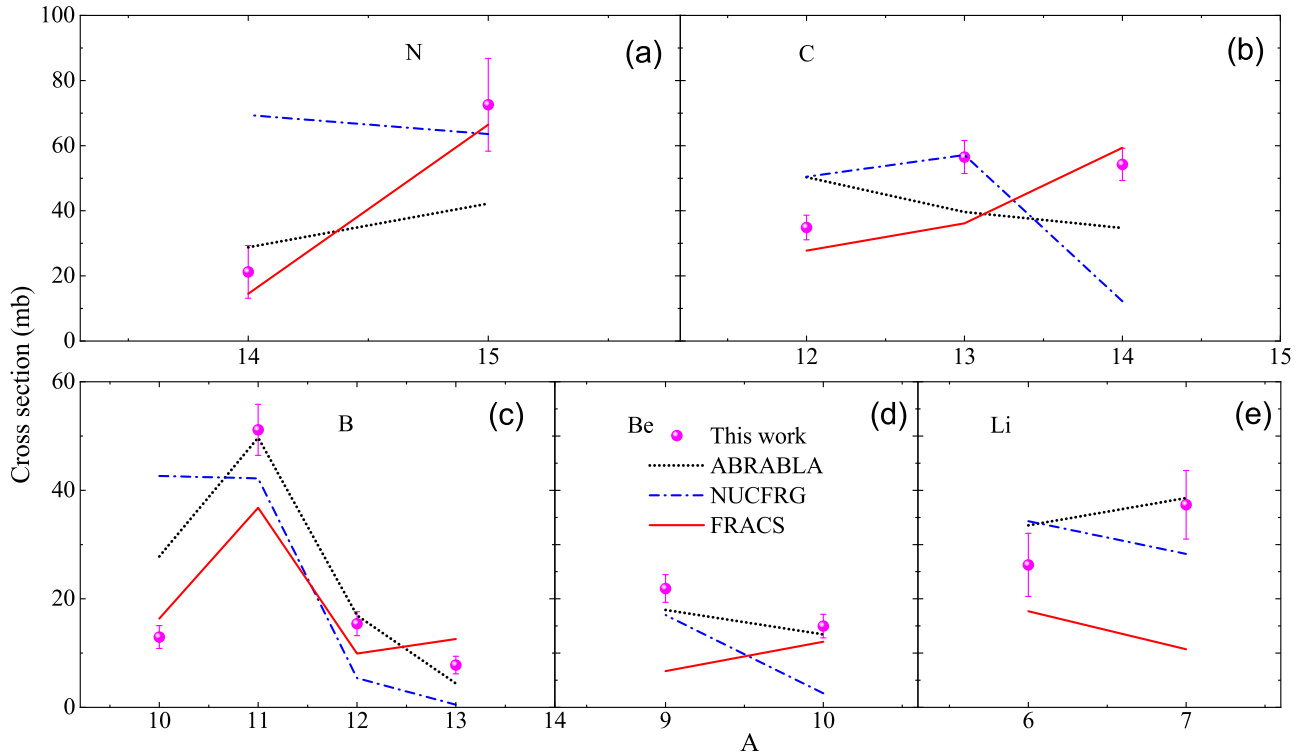


FIG. 8. Production cross sections of N, C, B, Be, and Li isotopes produced by ^{16}N fragmentation on a carbon target. Cross sections measured in this work are compared with calculations by different models, i.e., ABRABLA, NUCFRG, and FRACS.

Our experimental cross sections were also applied to validate three fragmentation models, i.e., ABRABLA, NUCFRG, and FRACS. These fragmentation model calculations agree with most of our experimental data within a factor of 2, although large discrepancies are also observed for some isotopic cross sections, especially for those produced by fragmentation of unstable projectiles ^{14}C and ^{16}N . More experimental cross sections from unstable projectiles are required to further benchmark fragmentation models.

ACKNOWLEDGMENTS

This work was supported by the National Natural Science Foundation of China (Grants No. 12005314, No. U1867214, and No. 11875302), the SYSU 100 Top Talents Program, the Heavy Ion Research Facility in Lanzhou (HIRFL), and the Open Research Project of Chinese Academy of Sciences, Guangdong Major Project of Basic and Applied Basic Research (No. 2021B0301030006).

- [1] O. B. Tarasov, D. J. Morrissey, A. M. Amthor, T. Baumann, D. Bazin, A. Gade, T. N. Ginter, M. Hausmann, N. Inabe, T. Kubo, A. Nettleton, J. Pereira, M. Portillo, B. M. Sherrill, A. Stolz, and M. Thoennessen, *Phys. Rev. Lett.* **102**, 142501 (2009).
- [2] O. B. Tarasov, M. Portillo, A. M. Amthor, T. Baumann, D. Bazin, A. Gade, T. N. Ginter, M. Hausmann, N. Inabe, T. Kubo, D. J. Morrissey, A. Nettleton, J. Pereira, B. M. Sherrill, A. Stolz, and M. Thoennessen, *Phys. Rev. C* **80**, 034609 (2009).
- [3] O. B. Tarasov, M. Portillo, D. J. Morrissey, A. M. Amthor, L. Bandura, T. Baumann, D. Bazin, J. S. Berryman, B. A. Brown, G. Chubarian, N. Fukuda, A. Gade, T. N. Ginter, M. Hausmann, N. Inabe, T. Kubo, J. Pereira, B. M. Sherrill, A. Stolz, C. Sumithrarachichi, M. Thoennessen, and D. Weisshaar, *Phys. Rev. C* **87**, 054612 (2013).
- [4] M. Mocko, M. B. Tsang, L. Andronenko, M. Andronenko, F. Delaunay, M. Famiano, T. Ginter, V. Henzl, D. Henzlová, H. Hua, S. Lukyanov, W. G. Lynch, A. M. Rogers, M. Steiner, A. Stolz, O. Tarasov, M.-J. van Goethem, G. Verde, W. S. Wallace, and A. Zalessov, *Phys. Rev. C* **74**, 054612 (2006).
- [5] C. Villagrasa-Canton, A. Boudard, J. E. Ducret, B. Fernandez, S. Leray, C. Volant, P. Armbruster, T. Enqvist, F. Hammache, K. Helariutta, B. Jurado, M. V. Ricciardi, K. H. Schmidt, K. Summerer, F. Vives, O. Yordanov, L. Audouin, C. O. Bacri, L. Ferrant, P. Napolitani, F. Rejmund, C. Stephan, L. Tassan-Got, J. Benlliure, E. Casarejos, M. Fernandez-Ordenez, J. Pereira, S. Czajkowski, D. Karamanis, M. Pravikoff, J. S. George, R. A. Mewaldt, N. Yanasak, M. Wiedenbeck, J. J. Connell, T. Faestermann, A. Heinz, and A. Junghans, *Phys. Rev. C* **75**, 044603 (2007).
- [6] P. Napolitani, K. Schmidt, L. Tassan-Got, P. Armbruster, T. Enqvist, A. Heinz, V. Henzl, D. Henzlova, A. Kelic, R. Pleskac, M. V. Ricciardi, C. Schmitt, O. Yordanov, L. Audouin, M. Bernas, A. Lafriashk, F. Rejmund, C. Stephan, J. Benlliure, E. Casarejos *et al.*, *Phys. Rev. C* **76**, 064609 (2007).

- [7] D. Henzlova, K. H. Schmidt, M. V. Ricciardi, A. Kelic, V. Henzl, P. Napolitani, L. Audouin, J. Benlliure, A. Boudard, E. Casarejos, J. E. Ducret, T. Enqvist, A. Heinz, A. Junghans, B. Jurado, A. Krasa, T. Kurtukian, S. Leray, M. F. Ordonez, J. Pereira, R. Pleskac, F. Rejmund *et al.*, *Phys. Rev. C* **78**, 044616 (2008).
- [8] V. Föhr, A. Bacquias, E. Casarejos, T. Enqvist, A. R. Junghans, A. Kelić-Heil, T. Kurtukian, S. Lukić, D. Pérez-Loureiro, R. Pleskač, M. V. Ricciardi, K.-H. Schmidt, and J. Taïeb, *Phys. Rev. C* **84**, 054605 (2011).
- [9] J. Alcántara-Núñez *et al.*, *Phys. Rev. C* **92**, 024607 (2015).
- [10] H. Suzuki *et al.*, *Nucl. Instrum. Methods Phys. Res., Sect. B* **317**, 756 (2013).
- [11] O. B. Tarasov, D. S. Ahn, D. Bazin, N. Fukuda, A. Gade, M. Hausmann, N. Inabe, S. Ishikawa, N. Iwasa, K. Kawata, T. Komatsubara, T. Kubo, K. Kusaka, D. J. Morrissey, M. Ohtake, H. Otsu, M. Portillo, T. Sakakibara, H. Sakurai, H. Sato, B. M. Sherrill *et al.*, *Phys. Rev. Lett.* **121**, 022501 (2018).
- [12] D. S. Ahn, N. Fukuda, H. Geissel, N. Inabe, N. Iwasa, T. Kubo, K. Kusaka, D. J. Morrissey, D. Murai, T. Nakamura, M. Ohtake, H. Otsu, H. Sato, B. M. Sherrill, Y. Shimizu, H. Suzuki, H. Takeda, O. B. Tarasov, H. Ueno, Y. Yanagisawa, and K. Yoshida, *Phys. Rev. Lett.* **123**, 212501 (2019).
- [13] T. Ohnishi *et al.*, *J. Phys. Soc. Jpn.* **77**, 083201 (2008).
- [14] T. Ohnishi *et al.*, *J. Phys. Soc. Jpn.* **79**, 073201 (2010).
- [15] B. Mei *et al.*, *Nucl. Instrum. Methods Phys. Res., Sect. A* **624**, 109 (2010).
- [16] B. Mei, H. S. Xu, X. L. Tu, Y. H. Zhang, Y. A. Litvinov, K. H. Schmidt, M. Wang, Z. Y. Sun, X. H. Zhou, Y. J. Yuan, M. V. Ricciardi, A. Kelic-Heil, R. Reifarh, K. Blaum, R. S. Mao, Z. G. Hu, P. Shuai, Y. D. Zang, X. W. Ma, X. Y. Zhang, J. W. Xia *et al.*, *Phys. Rev. C* **89**, 054612 (2014).
- [17] B. Mei, H. S. Xu, Y. H. Zhang, M. Wang, X. L. Tu, K. H. Schmidt, Y. A. Litvinov, Z. Y. Sun, X. H. Zhou, Y. J. Yuan, K. Blaum, M. V. Ricciardi, A. Kelic-Heil, R. S. Mao, Z. G. Hu, P. Shuai, Y. D. Zang, X. W. Ma, X. Y. Zhang, J. W. Xia *et al.*, *Phys. Rev. C* **94**, 044615 (2016).
- [18] X. H. Zhang, Z. Y. Sun, R. F. Chen, Z. Q. Chen, Z. Y. Guo, J. L. Han, Z. G. Hu, T. H. Huang, R. S. Mao, Z. G. Xu, M. Wang, J. S. Wang, Y. Wang, G. Q. Xiao, H. S. Xu, X. H. Yuan, H. B. Zhang, X. Y. Zhang, and T. C. Zhao, *Phys. Rev. C* **85**, 024621 (2012).
- [19] B. Mei, J. Tu, X. Zhang, S. Wang, Y. Guan, Z. Mai, N. Zeng, X. Tu, Z. Sun, S. Tang, Y. Yu, F. Fang, D. Yan, S. Jin, Y. Zhao, S. Ma, and Y. Zhang, *Phys. Rev. C* **105**, 064604 (2022).
- [20] T. Baumann, M. Hausmann, B. M. Sherrill, and O. B. Tarasov, *Nucl. Instrum. Methods Phys. Res., Sect. B* **376**, 33 (2016).
- [21] T. Nilsson, *Eur. Phys. J. Spec. Top.* **156**, 1 (2008).
- [22] J. C. Yang *et al.*, *Nucl. Instrum. Methods Phys. Res., Sect. B* **317**, 263 (2013).
- [23] J. M. Kidd, P. J. Lindstrom, H. J. Crawford, and G. Woods, *Phys. Rev. C* **37**, 2613 (1988).
- [24] W. R. Webber, J. C. Kish, and D. A. Schrier, *Phys. Rev. C* **41**, 547 (1990).
- [25] T. Ogawa, T. Sato, S. Hashimoto, D. Satoh, S. Tsuda, and K. Niita, *Phys. Rev. C* **92**, 024614 (2015).
- [26] V. Panin *et al.*, *Phys. Lett. B* **797**, 134802 (2019).
- [27] J. M. Boillos *et al.*, *Phys. Rev. C* **105**, 014611 (2022).
- [28] R. Thies *et al.*, *Phys. Rev. C* **93**, 054601 (2016).
- [29] B. Mei, *Phys. Rev. C* **95**, 034608 (2017).
- [30] B. Mei, X. L. Tu, and M. Wang, *Phys. Rev. C* **97**, 044619 (2018).
- [31] B. Mei, *Phys. Rev. C* **100**, 054619 (2019).
- [32] K. Sümmerer, *Phys. Rev. C* **86**, 014601 (2012).
- [33] J. J. Gaimard and K. H. Schmidt, *Nucl. Phys. A* **531**, 709 (1991).
- [34] J. W. Wilson *et al.*, *Nucl. Instrum. Methods Phys. Res., Sect. B* **94**, 95 (1994).
- [35] O. B. Tarasov and D. Bazin, *Nucl. Instrum. Methods Phys. Res., Sect. B* **204**, 174 (2003).
- [36] B. Mei, *Phys. Rev. C* **103**, 044610 (2021).
- [37] B. Mei, *Chin. Phys. C* **45**, 084109 (2021).
- [38] Y. Z. Sun *et al.*, *Nucl. Instrum. Methods Phys. Res., Sect. A* **927**, 390 (2019).
- [39] Y. Z. Sun *et al.*, *Nucl. Instrum. Methods Phys. Res., Sect. A* **985**, 164682 (2021).
- [40] Y. Z. Sun, S. T. Wang, Z. Y. Sun, X. H. Zhang, D. Yan, B. H. Sun, J. W. Zhao, Y. P. Xu, D. Y. Pang, Y. H. Yu, K. Yue, S. W. Tang, C. Dong, Y. X. Zhao, F. Fang, Y. Sun, Z. H. Cheng, X. M. Liu, P. Ma, H. R. Yang, C. G. Lu, and L. M. Duan, *Phys. Rev. C* **99**, 024605 (2019).
- [41] Y. X. Zhao, Y. Z. Sun, S. T. Wang, Z. Y. Sun, X. H. Zhang, D. Yan, D. Y. Pang, P. Ma, Y. H. Yu, K. Yue, S. W. Tang, S. M. Wang, F. Fang, Y. Sun, Z. H. Cheng, X. M. Liu, H. R. Yang, C. G. Lu, and L. M. Duan, *Phys. Rev. C* **100**, 044609 (2019).
- [42] Y. Z. Sun, S. T. Wang, Z. Y. Sun, X. H. Zhang, S. Y. Jin, Y. X. Zhao, D. Y. Pang, S. W. Tang, D. Yan, P. Ma, Y. H. Yu, K. Yue, F. Fang, Y. J. Zhang, C. G. Lu, and L. M. Duan, *Phys. Rev. C* **104**, 014310 (2021).
- [43] X.-D. Xu, Y.-Z. Sun, S.-T. Wang, B. Mei, S.-Y. Jin, X.-H. Zhang, Z.-Y. Sun, Y.-X. Zhao, S.-W. Tang, Y.-H. Yu, D. Yan, F. Fang, Y.-J. Zhang, and S.-B. Ma, *Chin. Phys. C* **46**, 111001 (2022).
- [44] D. L. Olson, B. L. Berman, D. E. Greiner, H. H. Heckman, P. J. Lindstrom, and H. J. Crawford, *Phys. Rev. C* **28**, 1602 (1983).